Journal of Biomolecular NMR **29:** 259–269, 2004.

Measurement of scaled residual dipolar couplings in proteins using variable-angle sample spinning

Nathalie Lancelot[a], Karim Elbayed[a], Alberto Bianco[b] & Martial Piotto[a,c]
[a]*Institut de Chimie, FRE 2446, 4 rue Blaise Pascal, Université Louis Pasteur, 67084 Strasbourg, France*
[b]*Institut de Biologie Moléculaire et Cellulaire, UPR 9021 CNRS, 15 rue René Descartes, 67000 Strasbourg, France*
[c]*Bruker Biospin, 34 rue de l'industrie, 67166 Wissembourg, France*

Received 17 September 2003; Accepted 30 January 2004

Key words: aligned media, bicelles, NMR, residual dipolar couplings, variable-angle sample spinning

Abstract

NMR spectra of ubiquitin in the presence of bicelles at a concentration of 25% w/v have been recorded under sample spinning conditions for different angles of rotation. For an axis of rotation equal to the magic angle, the ^{1}H/^{15}N HSQC recorded without any ^{1}H decoupling in the indirect dimension corresponds to the classical spectrum obtained on a protein in an isotropic solution and allows the measurement of scalar J-couplings $^1J_{NH}$. For an angle of rotation smaller than the magic angle, the bicelles orient with their normal perpendicular to the spinning axis, whereas for an angle of rotation greater than the magic angle the bicelles orient with their normal along the spinning axis. This bicelle alignment creates anisotropic conditions that give rise to the observation of residual dipolar couplings in ubiquitin. The magnitude of these dipolar couplings depends directly on the angle that the rotor makes with the main magnetic field. By changing this angle in a controlled manner, residual dipolar couplings can be either scaled up or down thus offering the possibility to study simultaneously a wide range of dipolar couplings in the same sample.

Introduction

The introduction of the measurement of residual dipolar couplings (RDCs) for structure determination in protein NMR by Prestegard (Tolman et al., 1995) and Bax (Tjandra and Bax, 1997; Tjandra et al., 1996) has been a major step to obtain a new class of structural constraints. In particular, the unique possibilities offered by this method to characterize long range order can be considered as the missing stone that was plaguing NOE-derived structures. In the case of the measurement of heteronuclear one-bond $^1D_{NH}$ residual dipolar couplings, ^{1}H/^{15}N HSQC experiments are usually recorded without ^{1}H-decoupling in the indirect dimension. The value measured in these spectra corresponds to the absolute value of the sum of the isotropic scalar J-coupling $^1J_{NH}$ and of the anisotropic residual dipolar coupling $^1D_{NH}$. In order to extract residual dipolar couplings, a second non-oriented sample is required. The most popular alignment media used are DMPC/DHPC bicelles (Bax and Tjandra, 1997; Tjandra and Bax, 1997), bacteriophages (Clore et al., 1998; Hansen et al., 1998a, b), purple membrane proteins (Koenig et al., 1999; Sass et al., 1999), alcohol mixtures (Ruckert and Otting, 2000) and polyacrylamide gels (Sass et al., 2000; Tycko et al., 2000). Whereas these alignment media provide adequate RDC values for $^1D_{NH}$, this is not the case for $^1D_{C'C\alpha}$, $^1D_{C'N}$ and $^2D_{C'HN}$ that have intrinsically lower values due to either the lower product of the gyromagnetic ratios involved or the longer internuclear distances. These weaker dipolar couplings are therefore difficult to measure and a high accuracy is required to obtain reliable structural information (Bax et al., 2001). Clearly, it would be of interest to work on slightly more oriented systems that would make these weak dipolar couplings larger and their measurement easier. At the same time, keeping the larger dipolar coupling constants like $^1D_{NH}$ to a reasonable value would also be desirable. A solution to this problem

would be to use a system leading to a slightly stronger alignment but where all the dipolar couplings could be scaled at will.

Following some earlier work on liquid crystals (Courtieu et al., 1994) and on bicelles (Sanders and Schwonek, 1992; Tian et al., 1999), we have investigated the possibilities offered by the system DMPC/DHPC bicelles at a concentration of 25% w/v associated with the techniques of variable-angle sample spinning. The behavior of liquid crystals orientation under variable angle spinning conditions has been studied extensively by Courtieu and coworkers (Courtieu et al., 1982, 1994) and their work has laid the foundation for the variable angle spinning experiments on bicelles performed more recently (Tian et al., 1999; Zandomeneghi et al., 2001). A bicelle possesses a negative anisotropy of the magnetic susceptibility ($\Delta\chi < 0$) and, when rotated around an axis making an angle θ with the magnetic field, the bicelle normal, also called director, orients perpendicular to the spinning axis when the angle of rotation θ is in the range $0° \leq \theta < 54.7°$. When the axis of rotation is comprised in the range $54.7° < \theta \leq 90°$, the bicelle normal becomes parallel to the axis of rotation (Tian et al., 1999; Zandomeneghi et al., 2001). At the exact magic angle ($\theta = 54.7°$), the bicelles lose their orientation and adopt an isotropic behavior with no privileged direction. This particular behavior allows therefore to study isotropic data and to obtain J-coupling at the magic angle, while spinning at angles different from the magic angle allows to measure residual dipolar couplings. Recently, experiments using this type of approach have been used by the group of Meier (Zandomeneghi et al., 2001, 2003a, b). Using switched-angle experiments, they were able to record, on a five amino acid membrane peptide, a $^1H/^1H$ correlation experiment where the indirect dimension is recorded at $\theta = 0°$ and the direct dimension is recorded at $\theta = 54.7°$.

In this paper, we present the first application of the combined use of variable-angle sample spinning and of the DMPC/DHPC bicelle system at a concentration of 25% v/w to the study of a soluble protein. We show that by using a high resolution magic angle spinning (HRMAS) probe (Lippens et al., 1999) and gradient $^1H/^{15}N$ HSQC experiments, we are able to extract isotropic $^1J_{NH}$ scalar couplings as well as residual heteronuclear $^1D_{NH}$ dipolar couplings whose amplitude can be scaled almost at will.

Material and methods

Sample preparation

Bicelles were prepared by mixing 50 mg of lipids (1,2-Dihexanoyl-*sn*-glycero3-phosphocholine (DHPC) and 1,2-Ditetradecanoyl-*sn*-glycero3-phosphocholine (DMPC), q=[DMPC]/[DHPC] =3) with 140 µl of phosphate buffer (10 mM phosphate buffer, 0.15 mM sodium azide, 90% H_2O, 10% D_2O, pH = 6.6). They were then carried through the following steps 5 times: vortexing (2 min), heating to 37 °C (20 min), vortexing (2 min), cooling to 0 °C (20 min). A 3,3 mM solution of ^{15}N-labelled ubiquitin was prepared in phosphate buffer and 60 µl of this solution were added to the bicelle solution. The sample was again carried through the procedure of vortexing, heating to 37 °C, vortexing and cooling to 0 °C (one time). The final sample concentration was 1.0 mM ubiquitin in 25% w/v bicelle solution (corresponding to 250 mg of lipids/ml). 50 µl of this solution were then transferred into a 4mm HRMAS rotor fitted with a Teflon insert in order to position all the sample within the detection volume of the solenoid coil. The total amount of ubiquitin present in the rotor was therefore 0.43 mg. ^{15}N-labelled ubiquitin was purchased from VLI Research Inc. and the lipids from Avanti Polar Lipids. Freshly prepared bicelle solutions were used for all experiments.

NMR experiments

NMR experiments were carried out on a 400 MHz Bruker Avance spectrometer equipped with a slightly modified gradient $^1H/^{15}N$ HRMAS probe (Lippens et al., 1999). This probe is designed with a stator that is able to flip from the vertical to the magic angle position in order to allow for the injection and ejection of the sample. It is therefore possible to envision some variable-angle sample spinning experiments on this type of probes. By slightly modifying the micrometer screw used to adjust precisely the magic angle, it becomes possible to have access to a range of angles comprised between 40° and 60°. All NMR experiments were carried out at a temperature of 308K and at a speed of 0 Hz (static conditions) or 800 Hz in order to obtain a stable homogeneous liquid crystal phase. $^1H/^{15}N$ HSQC experiments were recorded using the sensitivity improved acquisition scheme (Kay et al., 1992). The ^1H-coupled $^1H/^{15}N$ HSQC experiment differed from the ^1H-decoupled experiment simply by the omission of the 180° (^1H) pulse during the t1 evolution delay of the ^{15}N magnetization. 1 k complex

points were acquired in the acquisition dimension and 128 complex points were required in the indirect dimension. Sine-shaped gradient pulses of length 1.5 ms and of strength 40 G cm^{-1} and 4.04 G cm^{-1} were used to select the correct coherence order pathway. The length of the 90° proton pulse at $\theta = 54.7°$ was 8.7 μs. This value varied as a function of the angle θ in the following manner: $P_{90}(^1H) = 11.0$ μs at 41.8°, $P_{90}(^1H) = 9.5$ μs at 50.0° and $P_{90}(^1H) = 8.5$ μs at 57.0°.

The residual dipolar coupling under variable-angle sample spinning

Theory

A detailed description of the computation procedure used to calculate the expression of the residual dipolar constant for non-spinning samples in oriented media has been given by several authors (Bax et al., 2001; Fung, 1996; Prestegard et al., 1999, 2000). In the following, we present an analogous derivation for spinning oriented samples which follows a procedure previously used for liquid crystals (Courtieu et al., 1994; Emsley, 1996, 2002; Fung, 1996) and bicelles (Zandomeneghi et al., 2003).

In order to compute the behavior of residual dipolar couplings under variable angle spinning, it is necessary to perform a number of transformations to relate the principal axis system of the dipolar interaction (PAS) to the laboratory frame where the final NMR spectrum is computed. The various reference frames used in this calculation are represented in Figure 1. Each transformation between two different frames is described by a set of Euler angles noted $\Omega = (\alpha, \beta, \gamma)$.

The dipolar interaction is first described in the principal axis system (PAS) of the dipolar interaction (Frame $\mathbf{D}_{\mathrm{Dip}}$) which corresponds to the N-H bond in the case of a dipolar interaction between a ^1H_N and its directly bonded ^{15}N. Since the dipolar interaction is of axial symmetry, the only spatial component which is non-zero in Frame $\mathbf{D}_{\mathrm{Dip}}$ is $R_{2,0}^{\mathrm{D_{Dip}}}$ (Schmidt-Rohr and Spiess, 1999). The N-H bond might be endowed with some internal dynamics that makes the N-H bond position time-dependant. The purpose of the first transformation is therefore to relate the time-dependant position of the N-H vector to an average position described by a Frame $\mathbf{D}_{\mathrm{AV}}$. This transformation is characterized by the time-dependant Euler angle $\Omega_{\mathrm{D_{Dip}D_{AV}}}(t) = (\alpha_{\mathrm{D_{Dip}D_{AV}}}(t), \beta_{\mathrm{D_{Dip}D_{AV}}}(t), \gamma_{\mathrm{D_{Dip}D_{AV}}}(t))$. The Euler angle to be considered is therefore the average of all Euler angles.

$$\bar{\Omega}_{\mathrm{D_{Dip}D_{AV}}}(t) = \overline{(\alpha_{\mathrm{D_{Dip}D_{AV}}}(t), \beta_{\mathrm{D_{Dip}D_{AV}}}(t), \gamma_{\mathrm{D_{Dip}D_{AV}}}(t))}.$$

Mathematically, this transformation is represented by (Schmidt-Rohr and Spiess, 1999):

$$\begin{aligned} R_{2,m}^{\mathrm{D_{AV}}} &= \sum_{\mathrm{m'}=-2}^{+2} R_{2,m'}^{\mathrm{D_{Dip}}}\, \overline{D_{\mathrm{m',m}}^2(\Omega_{\mathrm{D_{Dip}D_{AV}}}(t))} \\ &= R_{2,0}^{\mathrm{D_{Dip}}}\, \overline{D_{0,m}^2(\Omega_{\mathrm{D_{Dip}D_{AV}}}(t))}, \end{aligned} \tag{1}$$

where $R_{2,m}^{\mathrm{D_{AV}}}$ represents the spatial components of the dipolar interaction in Frames $\mathbf{D}_{\mathrm{AV}}$ and

$$\overline{D_{\mathrm{m',m}}^2(\Omega_{\mathrm{D_{Dip}D_{AV}}}(t))}$$

is the average of the $D_{\mathrm{m',m}}^2$ Wigner function.

The only Wigner function that is relevant for axially symmetrical motion is

$$\overline{D_{0,0}^2(\Omega_{\mathrm{D_{Dip}D_{AV}}}(t))}.$$

This term is also called the generalized internal order parameter S (Lipari and Szabo, 1982) and quantifies the amount of internal dynamics. Equation 1 can therefore be rewritten as:

$$R_{2,0}^{\mathrm{D_{AV}}} = S\, R_{2,0}^{\mathrm{D_{Dip}}} \tag{2}$$

The second transformation leads to a molecular frame (Frame $\mathbf{M}$) which is fixed in the molecule. This transformation is characterized by the angle $\Omega_{\mathrm{D_{AV}M}} = (0, \beta_{\mathrm{D_{AV}M}}, \gamma_{\mathrm{D_{AV}M}})$. The first angle $\alpha_{\mathrm{D_{AV}M}}$ is equal to zero since the dipolar interaction is axially symmetrical and two Euler angles are sufficient to describe the rotation. Mathematically, this transformation is represented by:

$$R_{2,m}^{\mathrm{M}} = \sum_{\mathrm{m'}=-2}^{+2} R_{2,\mathrm{m'}}^{\mathrm{D_{AV}}}\, D_{\mathrm{m',m}}^2(\Omega_{\mathrm{D_{AV}M}}). \tag{3}$$

Since, according to Equation 2, only $R_{2,0}^{\mathrm{D_{AV}}}$ exists in frame $\mathbf{D}_{\mathrm{AV}}$, Equation 3 simplifies to:

$$\begin{cases} R_{2,0}^{\mathrm{M}} = R_{2,0}^{\mathrm{D_{AV}}}\, D_{0,0}^2(\Omega_{\mathrm{D_{AV}M}}) \\ R_{2,\pm2}^{\mathrm{M}} = R_{2,0}^{\mathrm{D_{AV}}}\, D_{0,\pm2}^2(\Omega_{\mathrm{D_{AV}M}}) \\ R_{2,\pm1}^{\mathrm{M}} = R_{2,0}^{\mathrm{D_{AV}}}\, D_{0,\pm1}^2(\Omega_{\mathrm{D_{AV}M}}), \end{cases} \tag{4}$$

where $R_{2,\mathrm{m}}^{\mathrm{M}}$ represents the spatial components of the dipolar interaction in Frame $\mathbf{M}$ and $D_{0,\mathrm{m}}^2(\Omega_{\mathrm{D_{AV}M}})$ is

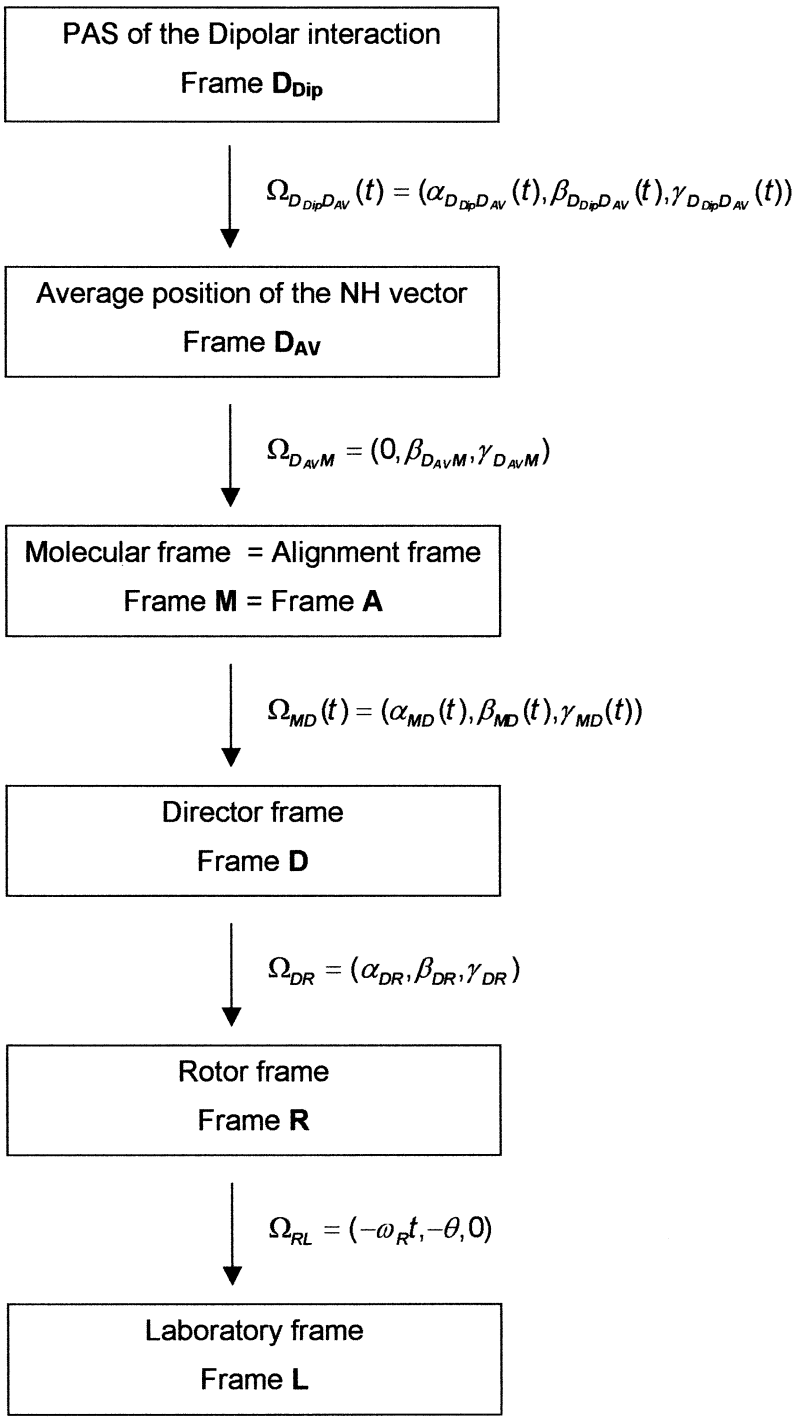

Figure 1. Reference frames used to compute the dipolar interaction in an oriented sample under variable-angle sample spinning.

the Wigner rotation matrix. The angles $\gamma_{D_{AV}M}$ and $\beta_{D_{AV}M}$ are important structural angles since they allow to position a given NH vector with respect to the molecular frame. The identification of these two angles is the final goal of the present procedure.

The third transformation allows to relate the molecular frame to the director frame (Frame **D**). This frame defines the most probable orientation of the bicelles. For example, in the case of a non-spinning bicelle, the Z axis of the director frame is perpendicular to the magnetic field B_0 since the bicelles tend to align with their normal perpendicular to B_0. This transformation is characterized by the time-dependant Euler angle $\Omega_{MD}(t) = (\alpha_{MD}(t), \beta_{MD}(t), \gamma_{MD}(t))$. At this stage, it is important to note that it is possible to choose the molecular frame **M** not in an arbitrary matter but as the principal axis system of the alignment tensor **A**. This is shown in Figure 1, where frame **M** is shown to coincide with frame **A**. In this case, the Saupe matrix (Saupe, 1968) that characterizes the alignment of the molecule in the director frame becomes diagonal and the only Wigner functions whose average is not zero are (Emsley, 1996, 2002):

$$\begin{cases} \overline{D^2_{0,0}(\Omega_{M,D}(t))} = S_{ZZ} = A_a \\ \overline{D^2_{\pm 2,0}(\Omega_{M,D}(t))} = \sqrt{\frac{1}{6}}(S_{XX} - S_{YY}) = \sqrt{\frac{3}{8}} A_r, \end{cases} \tag{5}$$

where A_a and A_r are the axial and radial component of the alignment tensor respectively. These two terms characterize the strength of the alignment. In a regular isotropic sample, they are both equal to zero. The transformation is therefore described by:

$$R^D_{2,0} = R^M_{2,0}\ A_a + \sqrt{\frac{3}{8}}(R^M_{2,+2} + R^M_{2,-2})\ A_r. \tag{6}$$

The fourth transformation leads to the rotor frame (Frame **R**) and is characterized by the Euler angle $\Omega_{DR} = (\alpha_{DR}, \beta_{DR}, \gamma_{DR})$.The transformation is represented by:

$$R^R_{2,m} = \sum_{m'=-2}^{+2} R^D_{2,m'}\ D^2_{m',m}(\Omega_{DR}). \tag{7}$$

In the case of a bicelle with a uniaxial director, the angle γ_{DR} can have any value between 0 and 2π. Equation 7 leads to:

$$\begin{cases} R^R_{2,0} &= R^D_{2,0}\ D^2_{0,0}(\Omega_{DR}) \\ R^R_{2,\pm 2} &= R^D_{2,0}\ D^2_{0,\pm 2}(\Omega_{DR}) \\ R^R_{2,\pm 1} &= R^D_{2,0}\ D^2_{0,\pm 1}(\Omega_{DR}). \end{cases} \tag{8}$$

The fifth and final transformation goes from the rotor frame to the laboratory frame (Frame **L**). In this frame, the only spin operator that defines the energy is $T^L_{2,0}$ and therefore the only spatial component is $R^L_{2,0}$. The two Euler angles involved are the angle θ between the rotation axis and B_0 as well as the angle $\omega_R t$, where ω_R represents the speed of rotation. The Euler angle is therefore $\Omega_{RL} = (-\omega_R t, -\theta, 0)$ and the transformation is described by:

$$\begin{aligned} R^L_{2,0} &= \sum_{m'=-2}^{+2} R^R_{2,m'}\ D^2_{m',0}(\Omega_{AR}) \\ &= R^R_{2,0}\ D^2_{0,0}(\Omega_{RL}) \\ &\quad + R^R_{2,+1}\ D^2_{+1,0}(\Omega_{RL}) \\ &\quad + R^R_{2,-1}\ D^2_{-1,0}(\Omega_{RL}) \\ &\quad + R^R_{2,+2}\ D^2_{+2,0}(\Omega_{RL}) \\ &\quad + R^R_{2,-2}\ D^2_{-2,0}(\Omega_{RL}) \end{aligned} \tag{9}$$

Using Equations 9, 8, 6, 5 and 3, and reintroducing the multiplicative factor corresponding to the static dipolar coupling constant provides the final expression for the residual dipolar coupling of an oriented medium spinning at an arbitrary angle expressed in units of Hz:

$$\begin{aligned} D_{Res} = \left(\frac{\mu_0}{4\pi}\right)\left(\frac{h}{2\pi}\right)\frac{\gamma_N\gamma_H}{\pi\, r^3_{NH}}\ S \\ \left[\frac{1}{2}(3\cos^2\beta_{D_{AV}A} - 1)A_a\right. \\ \left. + \frac{3}{4}A_r \sin^2\beta_{D_{AV}A}\ \cos(2\gamma_{D_{AV}A})\right] \\ \left[\frac{1}{4}(3\cos^2\theta - 1)(3\cos^2\beta_{DR} - 1)\right. \\ - \frac{3}{4}\sin 2\theta \sin 2\beta_{DR}\cos(\omega_R t + \gamma_{DR}) \\ \left. + \frac{3}{4}\sin^2\theta \sin^2\beta_{DR}\cos(2\omega_R t + 2\gamma_{DR})\right], \end{aligned} \tag{10}$$

where μ_0 is the magnetic permittivity of vacuum, h is the Planck's constant, γ_N and γ_H are the magnetogyric ratio of spin N and H respectively and r_{NH} is the distance between the two spins ^{15}N and ^1H. The prefactor

$$\left(\frac{\mu_0}{4\pi}\right)\left(\frac{h}{2\pi}\right)\frac{\gamma_N\gamma_H}{\pi\, r^3_{NH}}$$

corresponds to the static dipolar coupling constant D_{Static} expressed in Hz.

Equation 10 shows that under variable angle spinning, the residual dipolar interaction in an oriented sample like a protein-bicelle solution, is the product of the residual dipolar coupling usually observed in non-spinning samples (Bax et al., 2001) times a factor that is composed of a time-dependent and of a time-independent term. For a rotation axis oriented at the magic angle ($\theta = 54.7°$) or for a director whose Z axis is at an angle $\beta_{DR} = 54.7°$ with respect to the spinning axis, the time-independent term disappears and the dipolar coupling vanishes ie. $D_{Res} = 0$. One way of recovering the dipolar interaction is to recouple the interaction through the time-dependent terms $\omega_R t$ and $2\omega_R t$ using dedicated pulse sequences (Glaubitz et al., 2001; Trempe et al., 2002). An easier way to achieve the same goal is to spin the sample at an angle different from the magic angle ($\theta \neq 54.7°$). In that case, Equation 10 shows that the static residual dipolar coupling will be scaled by a factor λ given by:

$$\lambda = \frac{1}{4}\left(3\cos^2\theta - 1\right)\left(3\cos^2\beta_{DR} - 1\right) - \frac{3}{4}\sin 2\theta \sin 2\beta_{DR}\cos\left(\omega_R t + \gamma_{DR}\right) + \frac{3}{4}\sin^2\theta \sin^2\beta_{DR}\cos\left(2\omega_R t + 2\gamma_{DR}\right). \quad (11)$$

Taking into account only the time-independent term corresponding to the center-band leads to a scaling factor given by:

$$\lambda = \frac{1}{4}\left(3\cos^2\theta - 1\right)\left(3\cos^2\beta_{DR} - 1\right). \quad (12)$$

Equation 12 shows that the scaling factor is affected by the angle of rotation θ and by the angle β_{DR} that the director makes with the rotor axis. In the case of bicelles, β_{DR} also depends on θ.

Results and discussion

The speed of rotation plays a crucial role in variable-angle sample spinning experiments on bicelles. If the speed of rotation is too slow, the torque exerted by the rotor on the sample is too weak and the alignment of the bicelle director is not uniform. If the speed of rotation is excessive, multiple orientations occur complicating the extraction and analysis of the data. In accordance with previous studies, a value of 800 Hz was found to be adequate for our experiments (Courtieu et al., 1994; Zandomeneghi et al., 2001).

The first set of experiments was recorded with an angle of rotation equal to the magic angle ($\theta = 54.7°$).

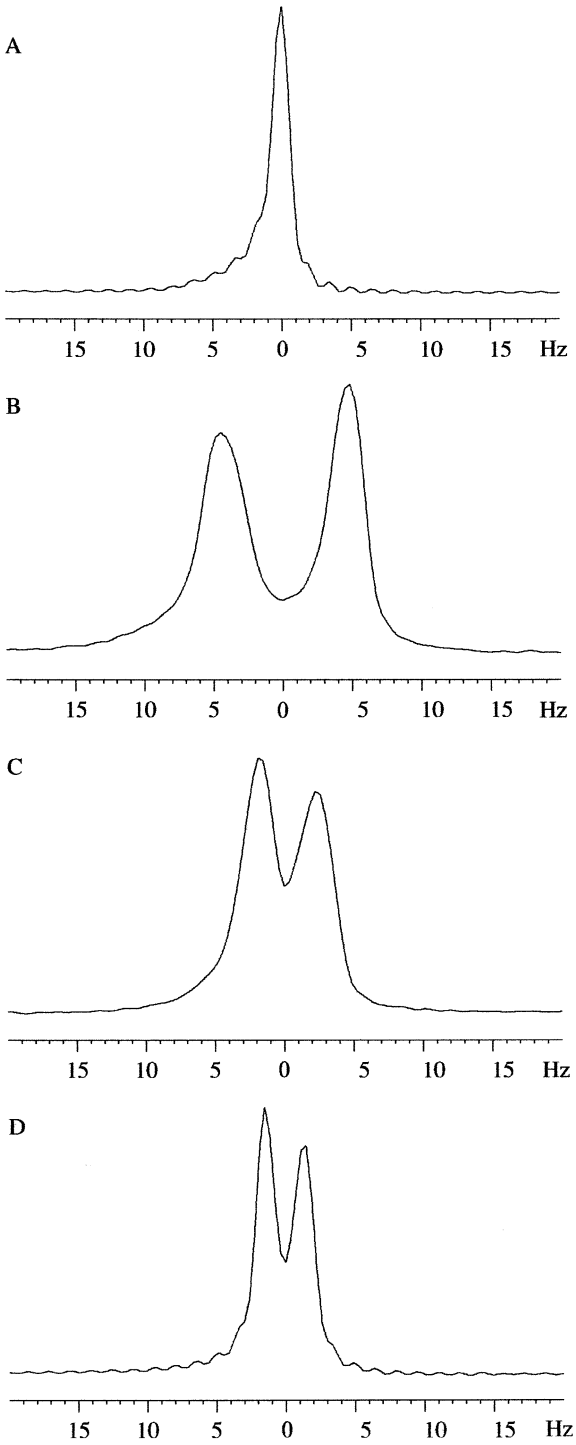

Figure 2. 1D deuterium spectrum of D_2O present in a sample of ubiquitin in bicelles in rotation at 800 Hz, at a temperature of 308 K and at different rotation angles: (A) 54.7° (B) 41.8° (C) 50.0° and (D) 57.0°.

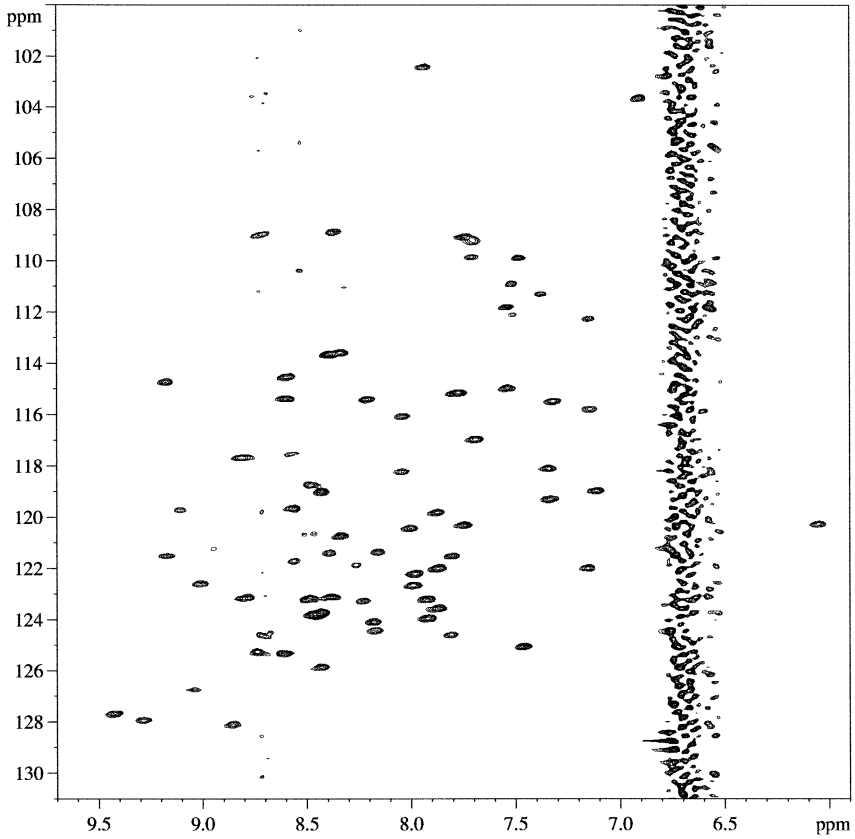

Figure 3. Ubiquitin in bicelles in rotation at the magic angle (54.7°) at a speed of 800 Hz and at a temperature of 308 K. 1H-decoupled $^{1}H/^{15}N$ HSQC: 16 transients were recorded for each of 256 increments in t1 corresponding to a total acquisition time of 1.3 h.

This angle allows to reproduce isotropic conditions by averaging out all the dipolar coupling constants to zero. The magic angle also averages out the first order quadrupolar coupling to zero allowing to obtain a singlet for the deuterium resonance of the D_2O molecules (Figure 2A). For bicelle samples the averaging of the dipolar and quadrupolar interactions by magic angle spinning is not strictly necessary since at the magic angle, the magnetic energy of the interaction of the bicelles with the magnetic field is zero and the bicelles are randomly distributed. In order to verify that, under the previous conditions, the sample behaves as described in the theoretical section, 2D $^{1}H/^{15}N$ HSQC experiments were recorded with and without ^{1}H decoupling in the indirect dimension. The ^{1}H-decoupled HSQC spectrum displays well resolved cross-peaks (Figure 3) that are similar to those obtained on a ubiquitin sample in solution without bicelles. An analysis of the ^{1}H linewidth of the HSQC cross-peaks recorded under magic angle spinning reveals that there is no significant difference between the experiment recorded on ubiquitin in bicelles and the one recorded on ubiquitin in solution. This observation shows that the presence of bicelles at a concentration of 25% w/v does not lead to an increase of the 1H-linewidth of ubiquitin thereby implying that the rotational correlation time of ubiquitin is not significantly modified by the presence of the bicelles. The S/N of the HSQC is quite high for a sample containing only 0.43 mg of ubiquitin recorded at 400 MHz and most of the resonances of ubiquitin can be attributed from this spectrum using literature values. A S/N calculation using a projection of the cross peaks gives an average value of about 27:1. Spinning at 800 Hz on a sample in 90% H_2O creates fairly intense spinning side-bands at $\pm$ 800 Hz around the water frequency obstructing part of the protein resonances. Side-bands of much lower intensity are also present at $\pm$ 1600 Hz. This effect is however not severe and, provided the sample rotation is stable enough, most of the resonances can be recovered. From the undecoupled HSQC spectrum scalar $^{1}J_{NH}$ couplings ranging from -91 to -96.5 Hz were extracted. These

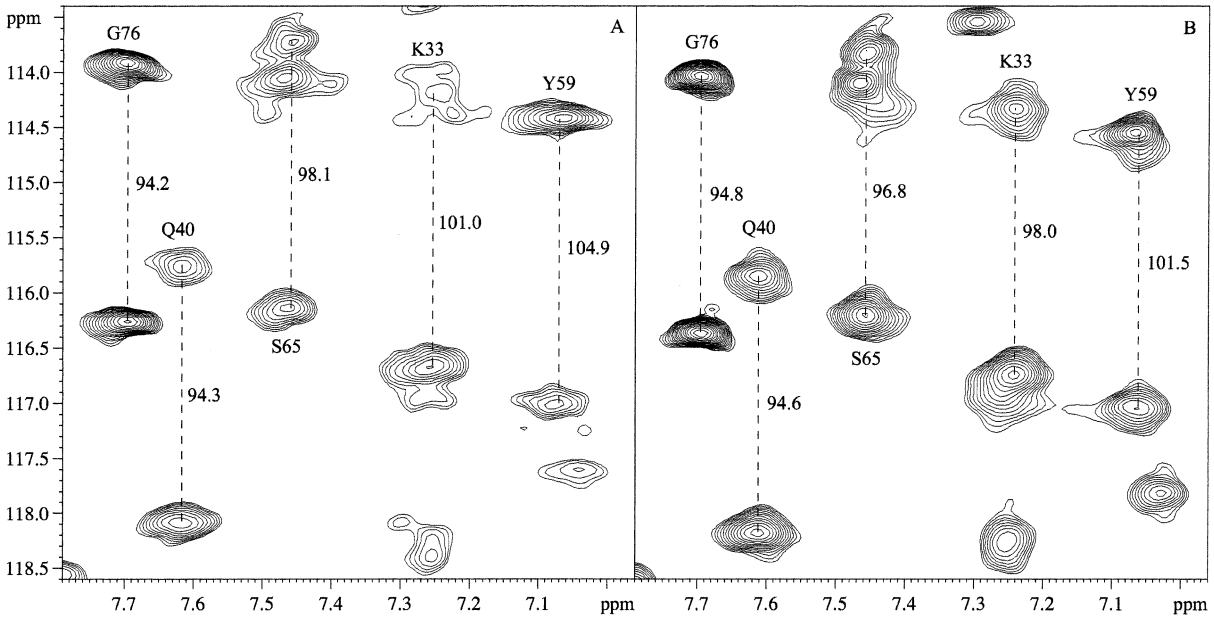

Figure 4. Ubiquitin in bicelles in rotation at a speed of 800 Hz and at a temperature of 308 K. (A) 1H-coupled $^{1}H/^{15}N$ HSQC spectrum at a rotation angle of 41.8°. Expansion showing characteristic scalar+dipolar coupling constants. Experimental time 10 h (B) 1H-coupled $^{1}H/^{15}N$ HSQC spectrum at a rotation angle of 57°. Expansion showing characteristic scalar+dipolar coupling constants. Experimental time 2 h.

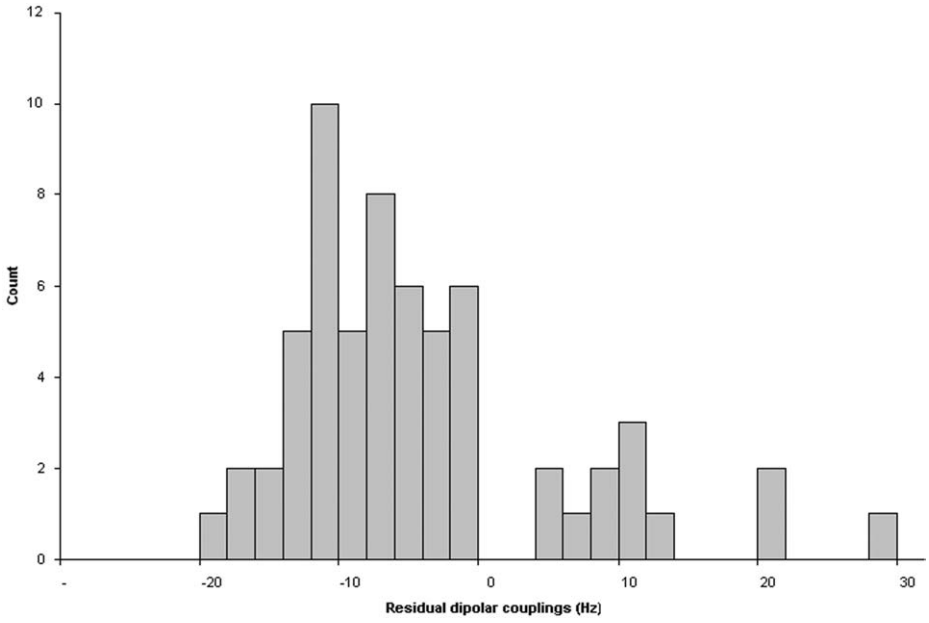

Figure 5. Distribution of the dipolar coupling constants $^{1}D_{NH}$ observed in the $^{1}H/^{15}N$ HSQC of ubiquitin in the presence of bicelles at a concentration of 25% w/v in rotation at a speed of 800 Hz and at an angle of 41.8° with respect to the magnetic field.

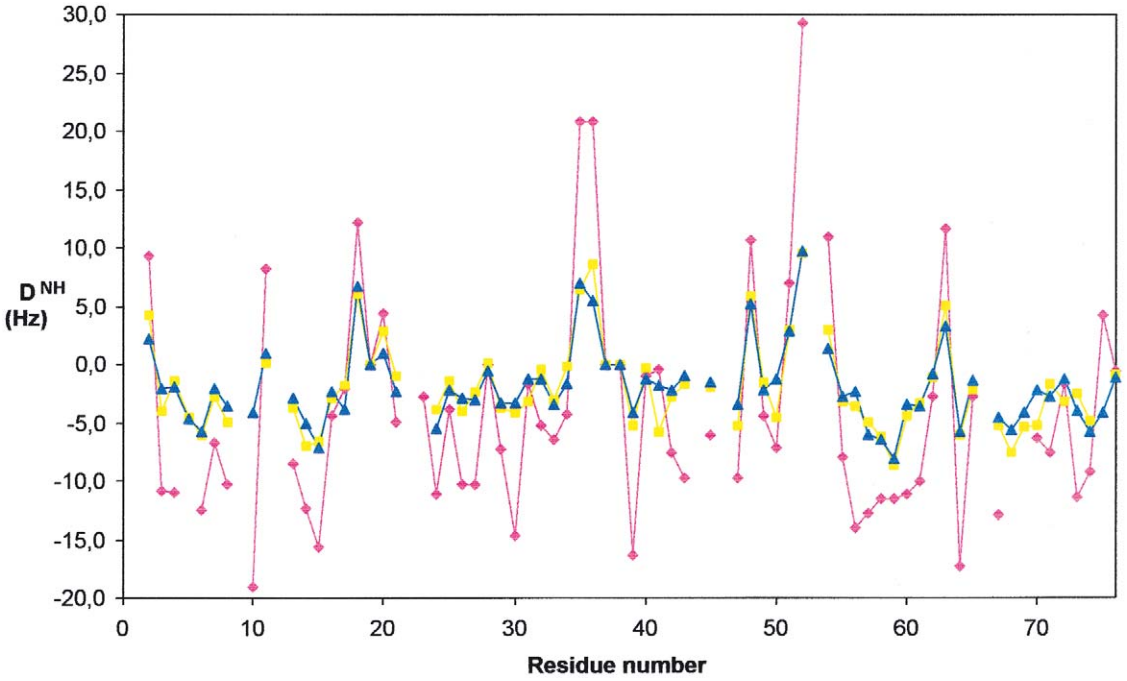

Figure 6. Representation of all the dipolar couplings $^{1}D_{NH}$ observed in the $^{1}H/^{15}N$ HSQC of ubiquitin in the presence of bicelles at a concentration of 25% w/v in rotation at a speed of 800 Hz and at the three following rotation angles: 41.8° (pink lozenges), 50° (yellow squares) and 57° (purple triangles).

values are very similar to the values published on ubiquitin in solution (Tjandra et al., 1996).

In a second step, the axis of rotation was changed to an angle of 41.8° with respect to the magnetic field. This value was measured by recording a 1D deuterium spectrum at a rotation of 800 Hz. Under these conditions, the D_2O molecules are partially oriented by the bicelles system and the deuterium quadrupolar coupling is not completely averaged out to zero leading to a sharp doublet (Figure 2B). For an angle $\Theta < 54.7°$ the ratio of the residual quadrupolar interaction over the static quadrupolar interaction is given by Equation 13 (Zandomeneghi et al., 2001):

$$\frac{\Delta\nu_{Res}}{\Delta\nu_{Static}} = -2\,\frac{(3\cos^2\beta_{DR}-1)}{2}\frac{(3\cos^2\theta-1)}{2} = \frac{(3\cos^2\theta-1)}{2}. \quad (13)$$

Under our experimental conditions, the static quadrupolar coupling is equal to 28 Hz, while the residual quadrupolar coupling of the spinning sample is equal to 9.5 Hz. By using Equation 13, the angle of rotation was computed to be about 41.8°. A point of practical interest here is that since the coil used in this study is a solenoid, the efficiency of the coil decreases as the coil is tilted towards the vertical position making pulses longer and sensitivity lower (see Material and methods section). The pulse length follows a $1/sin\theta$ dependence while the signal to noise follow therefore a $sin\theta$ dependence. The theoretical S/N at 41.8° is only equal to 81% of the S/N at 54.7°. The ^{1}H-decoupled HSQC obtained at this angle displays similar cross-peaks to those obtained at the magic angle. The HSQC cross peaks are only slightly broader in the ^{1}H dimension because of the presence of weak long range ^{1}H-^{1}H dipolar interactions and slightly poorer shimming. Indeed, it is known that for a spinning liquid sample confined within the detection volume of a coil, optimum shimming is obtained only at the magic angle (Barbara, 1994). A comparison of the ^{1}H-decoupled HSQC cross-peaks recorded at 54.7° and 41.8° shows that the linewidth increase is amino acid dependent with values comprised between +5% and +40% for ^{1}H and between +0% and +33% for ^{15}N. A similar analysis performed on the ^{1}H-coupled HSQC experiment leads to the same increase in ^{1}H linewidth while the ^{15}N linewidth of the slowly relaxing doublet component shows an increase comprised between 0% and 60%. The ^{1}H-coupled HSQC experiment obtained at 41.8° (Figure 4A) exhibits doublets in the f1 dimen-

sion that are markedly different from those recorded at the magic angle, ranging from +29.3 Hz to −19 Hz. This observation confirms the fact that off-magic angle spinning allows to recover part of the dipolar interaction induced by the bicelle alignment. Note that this value corresponds to a dipolar interaction scaled by a factor λ equal to −0.167 (Equation 12). The scaled RDC value of +29.3 Hz corresponds therefore to an unscaled value of −175 Hz. Using a rotation angle θ equal to 35° would give a corresponding dipolar coupling of 44.3 Hz. Most of the $^{1}H/^{15}N$ dipolar coupling constants could be extracted from this spectrum and the distribution of these values is shown in Figure 5.

Similar experiments were repeated at an angle of rotation of 50.0° and 57.0°. When taking the ratio of the values of the RDCs obtained at 41.8° and 50°, a fairly homogeneous value of 2.7 is obtained which is in good agreement with the value of 2.8 predicted by taking the ratio of the scaling factor λ (Equation 12). At an angle of 57°, the bicelles orientation changes by 90° resulting in a λ factor equal to −0.055. The ratio of the λ factor at 41.8° and 57° is equal to 3.0 which is again in agreement with the experimental ratio of 3.0. A comparison of all the unscaled RDCs obtained at the three different rotation angles is presented in Figure 6. The general aspect of this graph is in close agreement with the one previously published on ubiquitin in a 3.5% and 5% w/v DMPC/DHPC solution (Bax and Tjandra,1997). The previous results prove that, upon a change of the rotation angle, the alignment tensor does not change and that the residual dipolar coupling obtained at these different angles can be reliably compared and scaled to similar values taking as a correction factor the λ value. The dipolar couplings measured using these variable-angle sample spinning experiments are in good agreement with the ones obtained previously using static methods on ubiquitin in 5% w/v DMPC/DHPC bicelles (Cornilescu et al., 1998). The correlation coefficient for the data recorded at 41.8°, 50° and 57° is found to be equal to 0.95, 0.93 and 0.91 respectively. The variable-angle sample spinning technique described previously has the potential to measure easily RDCs of various magnitudes in a straightforward manner on a single protein sample. Scaling up dipolar couplings can help emphasize smaller RDCs and make their measurement more accurate. The accuracy of these measurements depends directly on the ^{15}N linewidth, however our experiments show that it increases only moderately when the axis of rotation is tilted from the magic angle to 41.8°. Moreover, since the line broadening observed in the ^{1}H-coupled HSQC experiment originates mainly from long range ^{1}H-^{15}N dipolar couplings with H_α and aliphatic protons, it is conceivable to selectively remove it by making use of band-selective decoupling at selected frequencies during the ^{15}N evolution time (Kooi et al., 1999). Such a scheme can also be used during ^{1}H acquisition to reduce the ^{1}H linewidth.

Conclusions

In this paper, we have demonstrated the first application of the combined use of variable-angle sample spinning and bicelles at a concentration of 25% w/v to the determination of residual dipolar couplings in a soluble protein. By using $^{1}H/^{15}N$ HSQC experiments we have shown that it is possible to manipulate easily the intensity of the dipolar coupling constants present in a protein by simply changing the axis of rotation of the sample. This procedure allows to use a single sample to simultaneously determine isotropic J-coupling values as well as residual dipolar couplings of different magnitudes in a single sample. Future applications could be the detection and measurement of smaller dipolar coupling constants like $^{1}D_{C'C\alpha}$, $^{1}D_{C'N}$ and $^{2}D_{C'HN}$ with a higher accuracy.

Acknowledgements

The authors wish to thank Christopher Aisenbrey for his assistance in preparing the DMPC/DHPC bicelles and André Walter for modifying the HRMAS probe used in this study.

Supporting information available

One table containing the ubiquitin $^{1}D_{NH}$ residual dipolar couplings obtained at 308 K and at a speed of 800 Hz at the following rotation angles: 41.8°, 50° and 57°.

References

Barbara, T.M. (1994) *J. Magn. Reson.*, **109**, 265–269.
Bax, A. and Tjandra, N. (1997) *J. Biomol. NMR*, **10**, 289–292.
Bax, A., Kontaxis, G. and Tjandra, N. (2001) *Meth. Enzymol.*, **339**, 127–174.
Clore, G.M., Starich, M.R. and Gronenborn, A.M. (1998) *J. Am. Chem. Soc.*, **120**, 10571–10572.

Cornilescu, G., Marquardt, J.L., Ottiger, M. and Bax, A. (1998) *J. Am. Chem. Soc.*, **120**, 6836–6837.

Courtieu, J., Alderman, D.W., Grant, D.M. and Bayles, J.P. (1982) *J. Chem. Phys.*, **77**, 723–730.

Courtieu, J., Bayle, J.P. and Fung, B.M. (1994) *Prog. Nucl. Magn. Reson. Spectrosc.*, **26**, 141–169.

Emsley, J.W. (1996) In *Encyclopedia of Nuclear Magnetic Resonance*, Vol. 4, Grant, D.M. and Harris, R.K. (eds.), Wiley, Chichester, pp. 2788–2799.

Emsley, J.W. (2002) In *Solid-State NMR Spectroscopy Principles and Applications*, Durer, M.J. (Ed.), Blackwell Science, Oxford, pp. 512–562.

Fung, B.M. (1996) In *Encyclopedia of nuclear magnetic resonance*, *Vol. 4*, Grant, D.M. and Harris, R.K. (Eds), Wiley, Chichester, pp. 2744–2751.

Glaubitz, C., Carravetta, M., Eden, M. and Levitt, M.H. (2001) In *Perspectives on Solid State NMR*, Kiihne, S.R. and de Groot, H.J.M. (Eds.), Kluwer Academic Publishers, Dordrecht, pp. 71–81.

Hansen, M.R., Mueller, L. and Pardi, A. (1998a) *Nat. Struct. Biol.*, **5**, 1065–1074.

Hansen, M.R., Rance, M. and Pardi, A. (1998b) *J. Am. Chem. Soc.*, **120**, 11210–11211.

Kay, L.E., Keifer, P. and Saarinen, T. (1992) *J. Am. Chem. Soc.*, **114**, 10663–10665.

Koenig, B.W., Hu, J.-S., Ottiger, M., Bose, S., Hendler, R.W. and Bax, A. (1999) *J. Am. Chem. Soc.*, **121**, 1385–1386.

Kooi, C.W.V., Kupce, E., Zuiderweg, E.R.P. and Pellecchia, M. (1999) *J. Biomol. NMR*, **15**, 335–338.

Lipari, G. and Szabo, A. (1982) *J. Am. Chem. Soc.*, **104**, 4546–4559.

Lippens, G., Bourdonneau, M., Dhalluin, C., Warras, R., Richert, T., Seetharaman, C., Boutillon, C. and Piotto, M. (1999) *Curr. Org. Chem.*, **3**, 147–169.

Prestegard, J.H., Al-Hashimi, H.M. and Tolman, J.R. (2000) *Q. Rev. Biophys.*, **33**, 371–424.

Prestegard, J.H., Tolman, J.R., Al-Hashimi, H.M. and Andrec, M. (1999) In *Biological Magnetic Resonance*, Vol. 17, Krishna, N.R. and Berliner, L.J. (Eds.), Kluwer Academic Publishers, London, pp. 311–355.

Ruckert, M. and Otting, G. (2000) *J. Am. Chem. Soc.*, **122**, 7793–7797.

Sanders, C.R. and Schwonek, J.P. (1992) *Biochemistry*, **31**, 8898–8905.

Sass, H.-J., Musco, G., Stahl, S.J., Wingfield, P.T. and Grzesiek, S. (2000) *J. Biomol. NMR*, **18**, 303–309.

Sass, J., Cordier, F., Hoffmann, A., Rogowski, M., Cousin, A., Omichinski, J.G., Lowen, H. and Grzesiek, S. (1999) *J. Am. Chem. Soc.*, **121**, 2047–2055.

Saupe, A. (1968) *Angew. Chem. Int. Ed. Engl.*, **7**, 97.

Schmidt-Rohr, K. and Spiess, H.W. (1999) *Multidimensional Solid-State NMR and Polymers*, Academic Press, London.

Tian, F., Losonczi, J.A., Fischer, M.W.F. and Prestegard, J.H. (1999) *J. Biomol. NMR*, **15**, 145–150.

Tjandra, N. and Bax, A. (1997) *Science*, **278**, 1111–1114.

Tjandra, N., Grzesiek, S. and Bax, A. (1996a) *J. Am. Chem. Soc.*, **118**, 6264–6272.

Tjandra, N., Grzesiek, S. and Bax, A. (1996b) *J. Am. Chem. Soc.*, **118**, 9279–9287.

Tolman, J.R., Flanagan, J.M., Kennedy, M.A. and Prestegard, J.H. (1995) *Proc. Natl. Acad. Sci. USA*, **92**, 9279.

Trempe, J.-F., Morin, F., Xia, P., Marchessault, R. and Gehring, K. (2002) *J. Biomol. NMR*, **22**, 83–87.

Tycko, R., Blanco, F.J. and Ishii, Y. (2000) *J. Am. Chem. Soc.*, **122**, 9340–9341.

Zandomeneghi, G., Tomaselli, M., v. Beek, J.D. and Meier, B.H. (2001) *J. Am. Chem. Soc.*, **123**, 910–913.

Zandomeneghi, G., Tomaselli, M., Williamson, P.T.F. and Meier, B.H. (2003a) *J. Biomol. NMR*, **25**, 113–123.

Zandomeneghi, G., Williamson, P.T.F., Hunkeler, A. and Meier, B.H. (2003b) *J. Biomol. NMR*, **25**, 125–132.